Electronic Materials Letters, Vol. 4, No. 4 (2008), pp. 147-150

Magnetoresistance and Magnetization of Heteroepitaxial InMnP:Zn Layer

C. S. Park, Hyungjun Kim, and J. Y. Son*

Department of Materials Science and Engineering, Pohang University of Science and Technology (POSTECH),
San 31, Hyoja-dong, Nam-gu, Pohang 790-784, Korea

The InMnP:Zn epilayer grown by liquid phase epitaxy method showed a heteroepitaxial crystal structure with precipitates. The magnetoresistance of the InMnP:Zn epilayer demonstrated that the InMnP:Zn epilayer has intrinsic characteristics of a diluted magnetic semiconductor (DMS). The temperature dependence of magnetization showed a mixture of two phase transitions. The origins of these transitions are attributed to the fact that the carrier mediated DMS and the secondary phase make ferromagnetism possible in view of the magnetization curve and the electron diffraction pattern of transmission electron microscopy.

Keywords: InMnP:Zn, diluted magnetic semiconductor, liquid phase epitaxy

1. INTRODUCTION

Recently, much attention has been focused on the applications of magnetic semiconductors, i.e., diluted magnetic semiconductor (DMS) alloys, for spin-sensitive electronics.[1-7] In addition, the fundamental physical properties of such material systems are also interesting. In III-V semiconductors, it is well known that substituted Mn^{2+} ions act as acceptor and lead to local magnetic moment formation.[8] The holes-mediated interaction between the magnetic moments of Mn ions, correlating their orientation, makes ferromagnetism possible. The functional importance of the devices based on this system strongly depends on high Curie temperature and room-temperature operation for the magnetic spin alignments.[9,10]

InP is a useful compound semiconductor due to its excellent physical properties and good characteristics for application to various devices. Especially, InP is considered as a possible candidate as a DMS material according to a theoretical report.[7] Mn has been reported to be used for a deep acceptor in InP, in which Mn gives spin polarized electrons.[11,12] In this study, we report results on the high Curie temperature property of the InMnP:Zn epilayer and its phase transition mechanism, in which Zn was additionally doped as an acceptor to form carrier-mediated ferromagnetism. We measured the temperature-dependent magnetization of the InMnP:Zn epilayer. Two kinds of magnetization with different Curie temperatures, near 40 K and above 350 K, were observed for the first time.

*Corresponding author: sonjyson@postech.ac.kr

2. EXPERIMENTAL DETAILS

InMnP:Zn epilayers were grown by LPE on p-type Zn-doped InP(001) substrate. Before the growth of InP epilayer, the substrate was cleaned by trichloroethylene (TCE), ethanol, and methanol and rinsed in deionized water for 5 min. The solvent was 6 N In melt and InP bulk; Zn and Mn powders were added as dopants. After prebaking the In and InP melt at 657°C for 2 hr, an appropriate amount of Zn and Mn powders were added to the growth melt. The growth was performed at 637°C, with a one step cooling process. The composition was determined using energy dispersive X-ray spectroscopy (EDX) and the microstructure was analyzed by transmission electron microscopy. Magnetoresistance (MR) analysis was carried out using a superconducting quantum interference device (SQUID), to characterize the magnetic properties and the phase transition temperature of the InMnP:Zn epilayer.

3. RESULTS AND DISCUSSION

X-ray diffraction measurements (θ-2θ) have been performed in order to estimate the structural properties of the InMnP:Zn epilayers. The doping level of Mn was evaluated from the lattice constant change, which was estimated to be approximately ~3%, agreeing with the EDX measurements. Although the exact value was difficult to obtain due to the existence of an anomalous Hall effect, the carrier (hole) concentration of the InMnP:Zn epilayer was determined to be approximately ~10^{19} cm^{-3} from Hall measurements at room temperature. Figure. 1 shows the electron diffraction pattern and plan view image of transmission electron microscopy

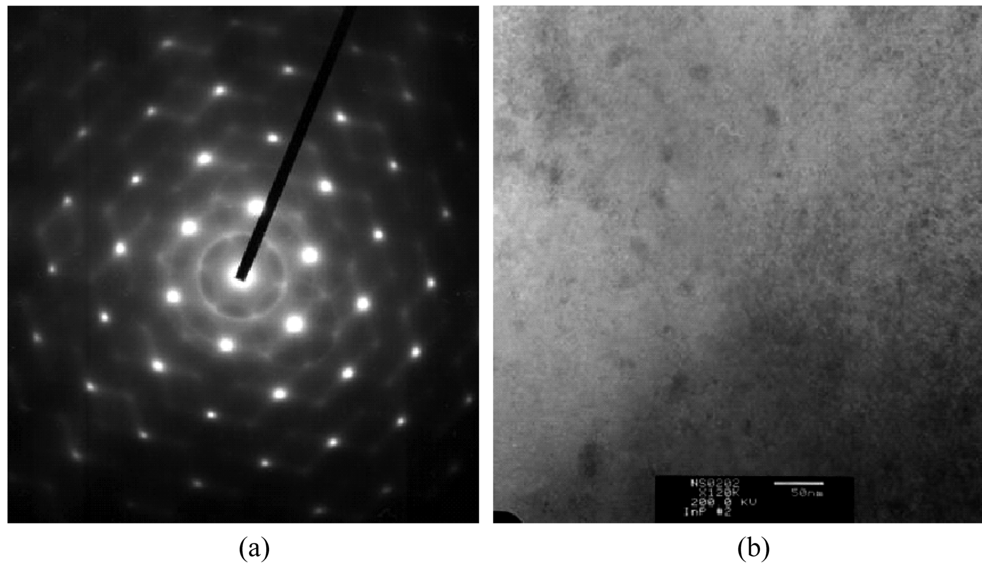

(a) (b)

Fig. 1. (a) Electron diffraction pattern and (b) plan view image from the transmission electron microscopy.

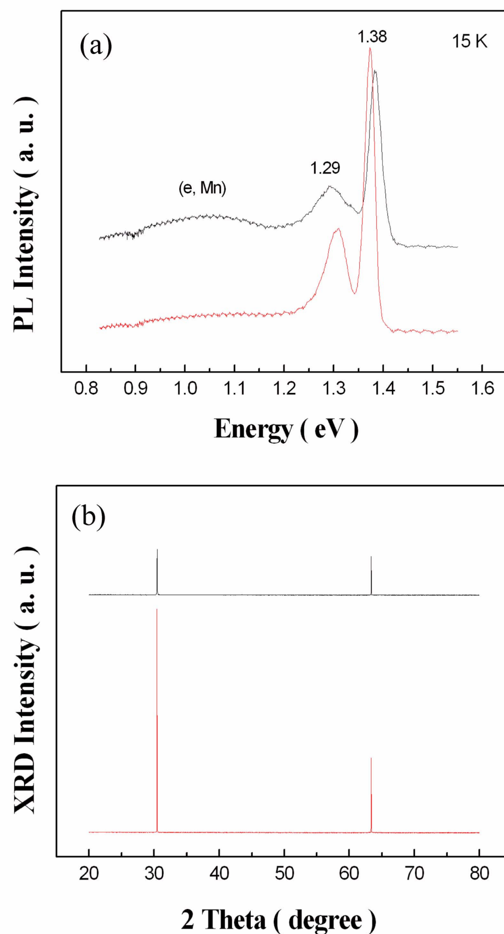

Fig. 2. PL spectra measured for the (In, Mn)P film with x 3% at 15 K; inset shows the XRD patterns, (002) and (004) of (In, Mn)P. Upper spectrum indicates film with precipitates; lower spectrum indicates film without precipitates.

(TEM). These images show that the InMnP:Zn epilayer has a heteroepitaxial crystallinity. Mn precipitates in the InP matrix, shown as dark regions, are created by the manganese segregation caused by the solubility limit of Mn.

Figure 2a shows the photoluminescence spectrum of the $In_{0.97}Mn_{0.03}P$ epilayer co-doped with Zn at 15 K. The peak near 1.38 eV, which is usually referred to as the Al peak, appears in InP grown by various methods. Recently, this was attributed to the presence of carbon acting as an acceptor. With regard to the above transition, the first phonon replica appeared near 1.33 eV. The transition related to Zn appeared near 1.29 eV. The intensity of band luminescence related to Mn from 0.9 to 1.20 eV is low and the energy positions of impurities shift to lower energy regions due to the surface state, well known in InP; the emission related to Mn has a broad band. It has been reported that the intentionally-doped InP:Mn has a higher Mn emission than it does band-related emission spectra.[13]

In our results, it is considered that there is a similar mechanism for the extinction of free carriers through nonradiative recombination via deep levels because of low intensity, although Mn is intentionally doped.[12] The high density of carriers results in tunneling transport through thermal energy between two Mn acceptor levels. The tunneling probabilities increase as temperature increases. While the dominant process at low temperatures is hole trapping, that at relatively high temperatures is the transport of hole hopping through the tunneling process.[11] Furthermore, this variance of hole concentrations is consistent with the Hall resistance at room temperature, which shows a negative differential conductivity behavior with two energy levels. InP with the Mn concentration of high impurity is known to have a strong phonon replica, n=0, n=1 and n=2 ranging to 1.1-1.2 eV with

the contribution of coupled-band luminescence related to Mn.[14] We confirmed that the transition is ascribed to a well localized transition metal level, that is, ferromagnetic type Mn centers that possibly form in InP.[15] This is given by a following mechanism, $e^- + Mn^{3+}(3d^4) + h \rightarrow Mn^{2+}(3d^5) + h$, (bound hole binding energy=0.23 eV).

The x-ray diffraction pattern shows the only high intensity of InP (002) and (004) plane as seen in the Fig. 2b. The Hall resistance R_{Hall} of a magnetic thin film is conventionally observed to contain two distinct components. The first results from the normal Hall Effect, which is proportional to the applied magnetic field, H; the second, called the anomalous Hall contribution, is proportional to the magnetization:

$$R_{Hall} = R_0H + R_SM, \qquad (1)$$

where M is the magnetization, and R_0, R_s are the ordinary and the anomalous Hall coefficients, respectively. In general, the anomalous Hall Effect is a consequence of spin-orbit coupling in the system.

Figure 3 shows the field dependence of the low temperature magnetoresistance measurements. Here, the resistivity change ($\rho = (\rho(B)-\rho(0)))/\rho(0)$) of the sample was measured with the magnetic field perpendicular to the sample, where $\rho(B)$ is the resistivity of sample with applied magnetic field and $\rho(0)$ is the initial resistivity without magnetic fields. The results show negative magnetoresistance as a function of applied fields below 40 K. This is ascribed to spin scattering interactions between the localized magnetic moments of the Mn acceptors and the holes in an impurity band. The magnitude of the negative magnetoresistance decreases as the temperature increases.

Hysteresis in the magnetoresistance was observed at 5 K, which is evidence that remnant magnetization within the sample continues to decrease the resistivity of the sample when the magnetic field is removed. This behavior was

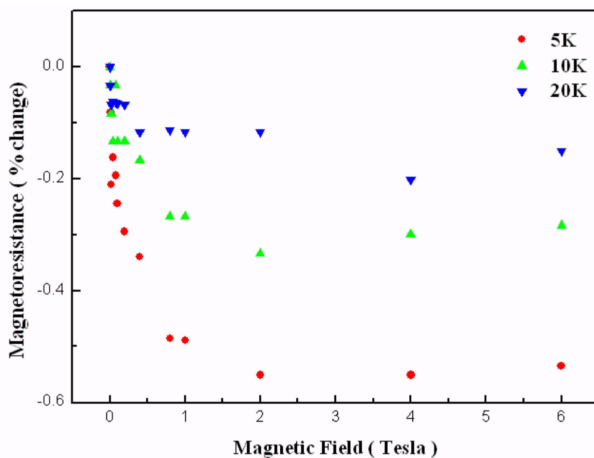

Fig. 3. Magnetoresistance measurements for the (In,Mn)P epilayer at low temperatures.

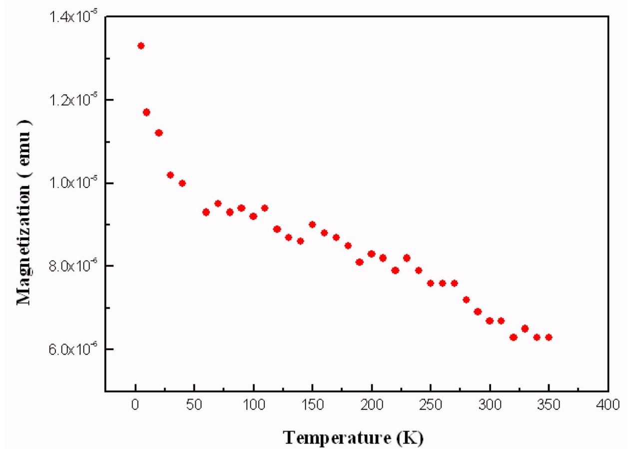

Fig. 4. Temperature dependence of magnetization for (In,Mn)P, obtained by SQUID with a magnetic field of 1000 Oe.

reported for InMnAs at 3.5 K by Ohno *et al.*[16] Curie point at low temperature range was found to be 40 K as determined from the maximum temperature at which the negative magnetoresistance is observed.[17]

Figure 4 shows the results of zero field cooled temperature-dependent magnetization using superconducting quantum interference device (SQUID). One transition temperature appears at above 350 K and another transition temperature near 40 K. It was reported that InMnP treated with various methods such as the implantation of Mn and the thermal diffusion of Mn has the same tendency of temperature dependence about Curie temperature.[18] In addition, the magnetic properties of p-type InMnP co-doped with Zn ($2.1\sim2.2\times10^{18}$ cm^{-3}) were previously reported.[18] For that study, Mn was evaporated on the top of InP:Zn(100) substrate fabricated using molecular beam epitaxy (MBE), after which the thermal diffusion of Mn was carried out by heat treatment. Phase transition occurs at above room temperature. In this study, two Curie temperatures were obtained, near 40 K and above 350 K, agreeing with our results for InMnP:Zn.

It is an interesting phenomenon that the transition temperature is shown in the high temperature region. We believe that the significant increase of Curie temperature from 40 K to 350 K originates from the distribution of secondary phase and MnP.[19] Even though the co-doping and the activation of Mn deep acceptors for the increase of Cure temperature is considered, the increasing value of Curie temperature is at most expected to the extent of 30 K through interlayer coupling.[20]

It is necessary to describe the secondary phases (precipitates) related to InMnP:Zn system to explain possible origins for the ferromagnetism. The possible precipitates in InMnP:Zn include MnP, Mn_2P, MnP_4, $InMn_3$, and Mn oxides (MnO, MnO_2, and Mn_2O_3). Such precipitates have their own magnetic ordering and are able to change the magnetic properties

of semiconductor host materials. MnP and Mn_2P demonstrate ferromagnetism with Curie temperature (T_c) at 291 K and antiferromagnetism with Neel temperature (T_N) at 103 K, respectively. Furthermore, $InMn_3$ is ferromagnetic up to the even relatively high temperature of 583 K. Therefore, high temperature ferromagnetism in Fig. 4 is considered due to $InMn_3$.

4. CONCLUSION

In conclusion, a heteroepitaxial InMnP:Zn layer on InP substrate was grown by LPE. The results of magnetoresistance and SQUID measurements well supported the idea that the InMnP:Zn epilayer is a ferromagnetic semiconductor. Temperature dependence of magnetization showed that the phase transition occurred at high T_C of above 350 K. Two mechanisms of phase transition, the intrinsic DMS phase and the secondary phase, exist in the InMnP:Zn epilayer according to InMnP and $InMn_3$, respectively.

ACKNOWLEDGEMENT

This work was supported by POSTECH Core Research Program, Korean Research Foundation Grant funded by the Korean Government (MOEHRD) (Grant No. KRF-2005-005-J13102) and the Brain Korea 21 project 2008.

REFERENCES

1. H. Munekata, H. Ohno, S. von Molnar, A. Segmuller, L. L. Chang, and L. Esaki, *Phys. Rev. Lett.* **63**, 1849 (1989).
2. H. Ohno, H. Munekata, T. Penney, S. von Molnar, and L. L. Chang, *Phys. Rev. Lett.* **68**, 2664 (1992).
3. J. De Boeck, R. Oesterholt, A. van Esch, H. Bender, C. Bruyseraede, C. Van Hoof, and G. Borghs, *Appl. Phys. Lett.* **68**, 2744 (1996).
4. H. Ohno, *Science* **281**, 951 (1998).
5. G. A. Prinz, *Science* **282**, 1660 (1998).
6. H. Shimizu, T. Hayashi, T. Nishinaga, and M. Tanaka, *Appl. Phys. Lett.* **74**, 398 (1999).
7. T. Dietl, H. Ohno, F. Matuskura, J. Cibert, and D. Ferrand, *Science* **287**, 1019 (2000).
8. S.-K. Choi, J. M. Jang, W.-G. Jung, J.-Y. Kim, and S.-D. Kim, *Electron. Mater. Lett.* **4**, 67 (2008).
9. Jin Seock Ma, Hyun Cheol Koo, Jongwha Eom, Joonyeon Chang, Suk-Hee Han, and Chulwoo Kim, *Electron. Mater. Lett*. **3**, 47 (2007).
10. Jinkwon Kim, Jongsoon Hong, and Kee Sun Lee, *Electron. Mater. Lett*. **3**, 169 (2007).
11. L. Eaves, A. W. Smith, M. S. Skolnick, and B. Cockayne, *J. Appl. Phys.* **53**, 4955 (1982).
12. Y. Ishitani, S. Minagawa, H. Hamada, and T. Tanaka, *J. Appl. Phys.* **82**, 1336 (1997).
13. L. Eaves, A. W. Smith, M. S. Skolnick, and B. Cockayne, *J. Appl. Phys.* **53**, 4955 (1982).
14. T. Takanohashi, T. Tanahashi, M. Sugawara, K. Kamite, and K. Nakajima, *J. Appl. Phys*. **63**, 1961 (1988).
15. Y. Shon, W. C. Lee, Y. S. Park, Y. H. Kwon, S. J. Lee, K. J. Chung, H. S. Kim, D.Y. Kim, D. J. Fu, T.W. Kang, X. J. Fan, Y. J. Park, and H. T. Oh, *Appl. Phys. Lett.* **84**, 2310 (2004).
16. H. Ohno, H. Munekata, S. von Molnar, and L. L. Chang, *J. Appl. Phys.* **69**, 6103 (1991).
17. R. P. Khoslar and J. R. Fischer, *Phys. Lett.* **32**A, 96 (1970).
18. Yoon Shon, H. C. Jeon, Y. S. Park, W. C. Lee, S. J. Lee, D. Y. Kim, H. S. Kim, H. J. Kim, T. W. Kang, Y. J. Park, Chong S. Yoon, and K. S. Chung, *Appl. Phys. Lett.* **85**, 1736 (2004).
19. E. E. Huber and D. H. Ridgley, *Phys. Rev.* **135**, A1033 (1964).
20. T. Jungwirth, W. A. Atkinson, B. H. Lee, and A. H. MacDonald, *Phys. Rev. B* **59**, 9818 (1999).